Dynamic Behaviour of Soils and Sub-Surface Ground

La Conduite Dynamique du Sol et le Sous-Sol

T.SHIBATA Professor,
T.SATO Assistant,
D.S.SOELARNO Graduate Student, Disaster Prevention Research Institute, Kyoto University, Japan

SYNOPSIS The first part of this paper considers the behaviour of soils under cyclic loading. The constitutive relation between the shear stress-strain and the effective confining pressure was proposed and checked by the dynamic triaxial tests. Then, the soil model was proposed to represent the equivalent shear modulus-strain-confining pressure relations for small strain level. In the second part, the behaviour of sub-surface ground during earthquake was analysed by using the proposed soil model and the wave propagation theory that have been obtained as the extension of the multiple reflection theory of wave. The recorded data during strong earthquake motions were used as an input for investigating the influence of non-linear behaviour of the soils on the stress and strain developed in the ground.

INTRODUCTION

For analysing the earthquake response of ground and foundation of structures, the dynamic behaviour of soil offers a key for solving the problems. The first part of this paper considers the dynamic stress-strain relations of soil on the point of view of effective stress. The soil model of hyperbolic type will be proposed, and the model is shown to simulate the behaviour of soils under the dynamic triaxial loading. Next, the authors reduce a simple stress-strain relation of soil which will be used to analyse the earthquake response of sub-surface ground.

A second purpose of this paper is to investigate the influce of non-linear properties of soil on the stress and strain developed in the ground during earthquake. In usual analysis, the multiple reflection theory or the lumped-mass method have been used. The multiple reflection theory, however, assumes the elastic half-space, and the lumped-mass method ignores the energy dissipation into the underlying half-space.

Considering the non-linearity of soil behaviour and the energy dissipation, the authors adapt the new wave propagation theory that had been obtained as the extension of the multiple reflection theory.

STRESS-STRAIN RELATION OF SOILS UNDER CYCLIC LOADING

The stress τ and strain γ in this paper are defined by the end points of hysteresis loops for different stress amplitudes. The curves through these end points look like ordinary stress-strain curves for a load increasing to failure. Hardin and Drnevich (1970) represented these curves by the hyperbolic equation as follows:

$$\frac{\tau}{\gamma} = \frac{G_o \gamma}{\tau_f + G_o \gamma} \quad \cdots\cdots\cdots\cdots\cdots\cdots (1)$$

where G_o is the initial shear modulus of soil and τ_f is the shear stress at failure.

For saturated soils which is consolidated isotropically by confining pressure σ_c and then cyclically loaded under undrained concition, effective mean principal stress σ'_m decreases from σ_c to σ'_m. The decreasing of σ'_m causes the reductions of both G_o and τ_f, and the authors assume the following relations.

$$\left.\begin{aligned} \frac{G_o}{\sigma_c} &= \alpha\left(\frac{\sigma'_m}{\sigma_c}\right)^m \\ \frac{\tau_f}{\sigma_c} &= \beta\left(\frac{\sigma'_m}{\sigma_c}\right)^n \end{aligned}\right\} \quad \cdots\cdots\cdots\cdots\cdots\cdots (2)$$

where α, β, m and n are the coefficients which depend on the soil type.

The above assumptions are explained by Fig.1. The value of σ'_m/σ_c in Fig.1 decreases from unity to zero during the undrained cyclic loading. The gradual decrements from G_{oi} and τ_{fi} to G_o and τ_f are treated by the coefficients m and n in Eq.(2), where G_{oi} and τ_{fi} in Fig.1 are the initial values of G_o and τ_f at $\sigma'_m=\sigma_c$. Concerning the coefficients α and β in Eq.(2), $\alpha=G_{oi}/\sigma_c$ and $\beta=\tau_{fi}/\sigma_c$ are obtained by substituting $\sigma'_m=\sigma_c$ into Eq.(2).

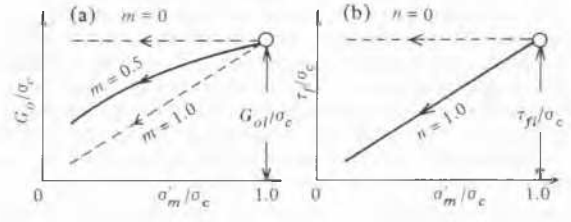

Fig.1 Explanation of Eq.(2)

Now, by substituting Eq.(2) into Eq.(1), τ-γ-σ'_m relation of soils may be expressed as

follows:

$$\left(\frac{\sigma_c}{\tau}\right)\gamma = \frac{1}{\alpha}\left(\frac{\sigma_c}{\sigma_m'}\right)^m + \frac{1}{\beta}\left(\frac{\sigma_c}{\sigma_m'}\right)^n \gamma \quad \cdots\cdots\cdots (3)$$

The values of m and n in Eq.(3) depend on the plasticity index of soil, e.g. highly plastic soil ; m = 0 and n = 0, cohesionless soil ; m = 0.5 and n = 1.0.

For sand, therefore, the stress-strain relation under cyclic loading may be obtained by substituting the values of m = 0.5 and n = 1.0 into Eq.(3) as follows:

$$\frac{\sigma_m'}{\tau} = \frac{1}{\beta} + \frac{1}{\alpha}\sqrt{\frac{\sigma_m'}{\sigma_c}} \cdot \frac{1}{\gamma} \quad \cdots\cdots\cdots\cdots (4)$$

DYNAMIC TRIAXIAL TESTS

A series of consolidated undrained dynamic triaxial tests was made for both saturated sands and undisturbed clays. In the test, the cyclic shear stress was applied by three kinds of loading, viz. axial stress σ_a -const., radial stress σ_r-const., and mean principal stress σ_m-const. Frequency range was below 6.0 Hz, and the excess pore-water pressure was measured at the bottom of the sample

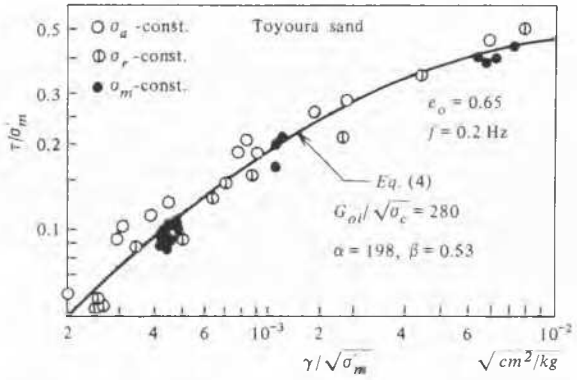

Fig.2 Stress-strain relation for sand

An example of test results on sand is shown in Fig.2 in the form of τ/σ_m' vs. $\gamma/\sqrt{\sigma_m'}$ plot. The different symbols correspond to the different loading method. The results shown in Fig.2 are scattered but Eq.(4) for sand seems to fit the experimental data.

SHEAR MODULUS AND DAMPING RATIO

In the preceding article the stress-strain relations under cyclic loading were considered on the basis of effective stress σ_m' as expressed by Eqs.(3) and (4). However, these results can not be used to analyse the practical problems, because of the difficulty of pore pressure estimation during the earthquake or vibration. In this article, therefore, the simple stress-strain relation of soils will be proposed for the case of no significant pore-water pressure develop.

Cohesionless soil: The following Eq.(5) may be obtained from Eq.(4) by setting $\sigma_m'=\sigma_c$ and $\alpha=G_{oi}/\sigma_c$,

$$\frac{\sqrt{\sigma_c}}{G} = \frac{\sqrt{\sigma_c}}{G_{oi}} + \frac{1}{\beta}\frac{\gamma}{\sqrt{\sigma_c}} \quad \cdots\cdots\cdots\cdots (5)$$

where $G=\tau/\gamma$ is the equivalent shear modulus.

Now, the resonant column test data obtained by Hardin and Drnevich (1970) are plotted in the form of $\sqrt{\sigma_c}/G$ vs. $\gamma/\sqrt{\sigma_c}$ in Fig.(3). From Fig.(3) it appears that the linear relationship between $\sqrt{\sigma_c}/G$ and $\gamma/\sqrt{\sigma_c}$ exists irrespective of the value of σ_c, and hence $G_{oi}/\sqrt{\sigma_c}$ and β in Eq.(5) can be determined.

The previous data of resonant column, simple shear and triaxial tests reported by others and the results of dynamic triaxial test by authors were plotted in the same form as shown in Fig.3. Then the values of $G_{oi}/\sqrt{\sigma_c}$ and β for each case are plotted in Fig.4 (the references on previous data are omitted from Fig.4 owing to limited space).

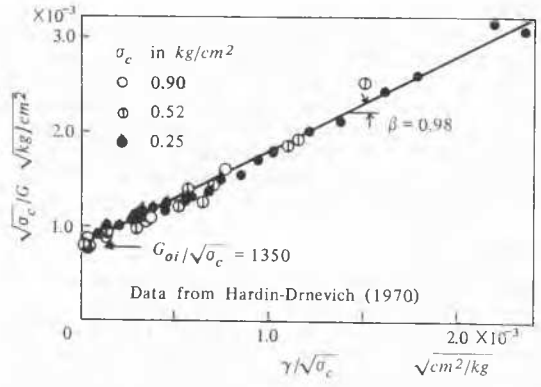

Fig.3 Determination of values of $G_{oi}/\sqrt{\sigma_c}$ and β

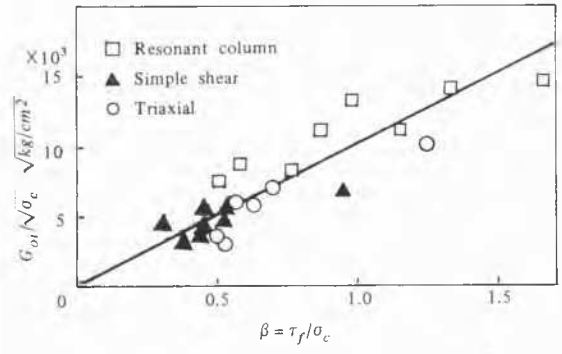

Fig.4 Relationship between $G_{oi}/\sqrt{\sigma_c}$ and β

The results shown in Fig.4 are scattered but they appear to indicate an increase of $G_{oi}/\sqrt{\sigma_c}$ for increased value of β. If it can be assumed that the linear relation between them exist as shown in Fig.4, we can get

$$G_{oi}/\sqrt{\sigma_c} = 10^3 \cdot \beta$$

where both G_{oi} and σ_c are in kg/cm^2.

Substituting the above relation into Eq.(5), the simple stress-strain relation for sand may be expressed as follows:

$$G_{oi}/G = 1 + 10^3 \cdot (\gamma/\sqrt{\sigma_c}) \cdots\cdots (6\text{-a})$$

Clay and Damping Ratio: Test data on clays were analysed by the same fashion as shown in Fig.4. The conclusion is that the simple

stress-strain relation for clay may be approximately expressed by Eq.(6-b),

$$G_{oi}/G = 1 + 3 \times 10^3(\gamma/\sqrt{\sigma_c}) \cdots\cdots\cdots (6\text{-b})$$

Concerning the damping ratio D of soils, Hardin and Drnevich (1970) proposed the following Eq.(7),

$$D = D_f\{1 - (G/G_{oi})\} \cdots\cdots\cdots\cdots (7)$$

In order to check the validity of Eq.(7), the values of D and G measured by the dynamic triaxial test on undisturbed clay are plotted in Fig.5. From this figure it appears that Eq.(7) fits the data.

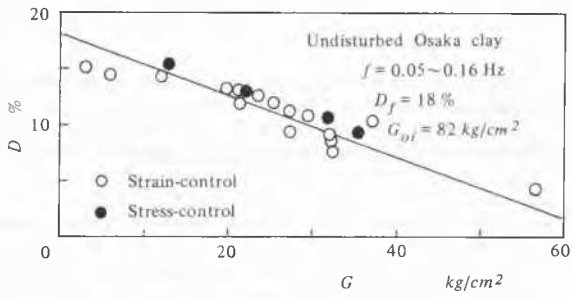

Fig.5 Damping ratio related to shear modulus

ANALYTICAL PROCEDURE OF GROUND BEHABIOUR DURING EARTHQUAKE

The equivalent shear modulus G and damping ratio D mentioned in the preceding article are expressed as a function of depth Z and strain amplitude $\gamma_o(Z)$.

$$G = G\{\gamma_o(Z), Z\} \ , \ D = D\{\gamma_o(Z), Z\} \cdots\cdots (8)$$

To formulate a non-linear harmonic wave solution in a material having properties expressed by Eq.(8), the surface layer is regarded as a kind of multi-layered system consisting of an infinite number of sub-layer with infinitesimally small thickness. Applying the multiple reflection theory to such a kind of multi-layered ground and letting the thickness of sub-layer to zero, Toki and Sato (1976) derived a non-linear harmonic wave solution as follows:

$$\left.\begin{aligned} U\{\gamma_o, Z, \omega\} &= f(\gamma_o, Z, \omega)\cdot F(\omega)/\omega \\ \Gamma\{\gamma_o, Z, \omega\} &= g(\gamma_o, Z, \omega)\cdot F(\omega)/\omega \end{aligned}\right\} \cdots\cdots (9)$$

where ω is a circular frequency, U and Γ are harmonic displacement and strain, respectively, $F(\omega)$ is a harmonic velocity at the ground surface and f and g are complicated function of γ_o, Z and ω.

In analysing the seismic response of surface layer using a non-linear harmonic wave solution expressed by Eq.(9), it is too difficult to estimate the value of $\gamma_o(Z)$. In this paper, the authors assume that $\gamma_o(Z)$ is defined as follows:

$$\gamma_o(Z) = C_o \cdot \tilde{\gamma}_o(Z) \cdots\cdots\cdots (10)$$

where C_o is an arbitrary constant and $\tilde{\gamma}_o(Z)$ is root mean square value of the shear strain at the depth Z:

$$\tilde{\gamma}(Z) = \sqrt{\frac{1}{T}\int_{-\infty}^{\infty} |\Gamma(\gamma_o, Z, \omega)|^2 d\omega} \cdots\cdots (11)$$

in which T is the time period of shear strain at the depth Z.

The stress and strain developed in the sub-surface ground during earthquake can be obtained by using Eqs.(9) and (10), but $\gamma_o(Z)$ can not be determined uniquely from Eqs.(10) and (11). In order to determine the value of $\gamma_o(Z)$, therefore, the usual repetitional calculations are made, and after the repetition of calculations $\gamma_o(Z)$ converges into the designated accuracy.

Once the Fourier transform of the recorded ground surface velocitygram is known, the deformation and strain in time domain at any depth can be readily evaluated by applying normal inverse transform procedures to Eq. (9). In this paper, the FFT algorithms are used for input data.

STRESS AND STRAIN DEVELOPED IN GROUND DURING EARTHQUAKE

Taft accelerogram (Hudson, et al 1971) was used to know how the stress and strain distributions in the sub-surface ground are affected by the non-linear behaviour of soils as expressed by Eqs.(6-a) and (7). In the analysis, shear modulus G_{oi} in these equation was assumed to vary as a function of depth (Sato, 1975). Fig.6(a) shows the maximum shear stress distributions within the sub-surface ground, and it will be seen that the stress distribution is not seriously affected by the non-linearity of the soil. On the other hand, the strain distribution is affected by the non-linearity and the value of C_o in Eq.(10) as shown in Fig.6(b).

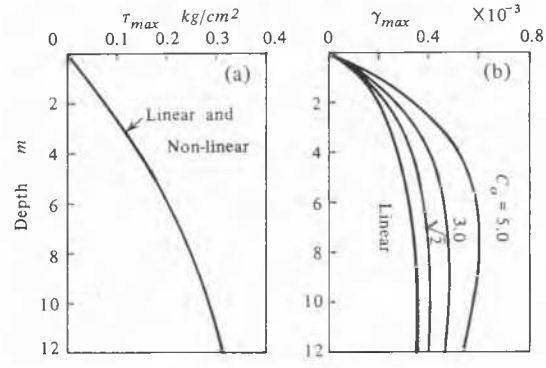

Fig.6 Effect of non-linearity of soil on stress and strain distributions

Fig.7 shows the effect of non-linear damping on the stress and strain distributions with depth. Solid and broken curves in Fig.7 correspond to D_f=0 and D_f=33%, where D_f is the damping ratio at failure as defined by Eq. (7). From Fig.7 it appears that the effect of non-linear damping on the stress and strain distributions is relatively unimportant for the case of Taft record.

Similar calculations as for Taft site were made by using the strong earthquake records obtained at four sites in Japan. To estimate the value of G_{oi} in Eq.(6-a), the in-situ shear wave velocities or N-values of S.P.T.

were used.

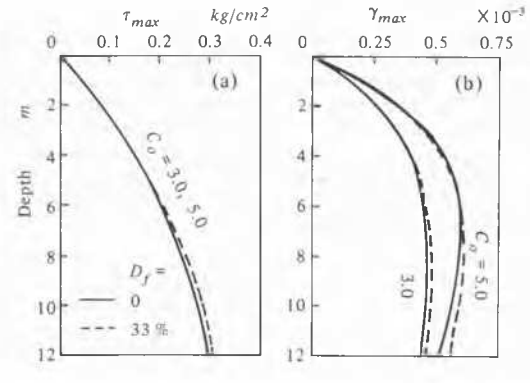

Fig.7 Effect of non-linear damping of soil on stress and strain distributions

Typical example of stress and strain distributions is shown in Fig.8. From this figure it seems that the strain calculated on the basis of non-linear behaviour of soils are twice to quadruple larger than that of linear case, but the stresses are unaffected by the non-linearity of soils. Almot the same characters as shown in Fig.8 were found for other three sites.

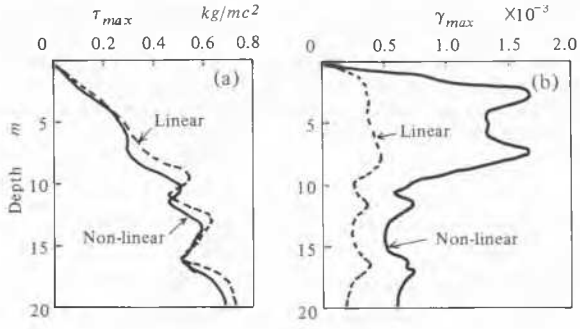

Fig.8 Stress and strain developed in the ground at Hachinohe site

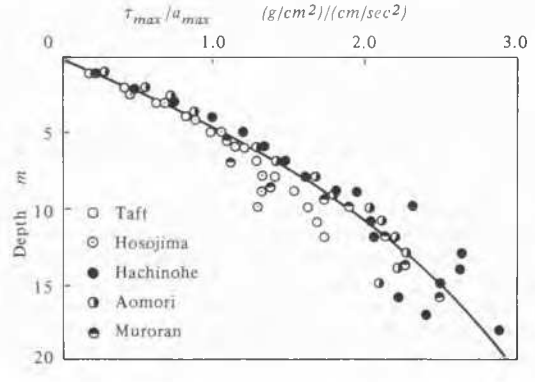

Fig.9 Ratio of the maximum shear stress at any depth and the maximum acceleration at surface

In Fig.9 are plotted the calculated ratios of τ_{max}/a_{max} for each site, where a_{max} is the recorded maximum acceleration at the ground surface. The results are scattered but they appear to indicate that the solid curve in Fig.9 may be used for the practical design purposes.

CONCLUSION

The constitutive equations (3) and (4) for soils under cyclic loading were proposed and checked by the dynamic triaxial undrained tests on saturated sands. Then, the equivalent shear modulus was related to the shear strain and confining presssure for convenient to use in the earthquake response analysis of sub-surface ground.

The effect of non-linearity of soil behaviour on the shear stress developed in the ground during earthquake was found to be relatively unimportant. For practical purposes, therefore, it will be allowed to use the stress values calculated from the linear theory. Concerning the strain in the ground, it seems more practical to calculate the strain from the constitutive equation of soils such as Eq.(6) by using the stress value estimated on the basis of linear theory.

The maximum shear stresses at any depth developed in the sub-surface ground during earthquake are roughly estimated by using the seismic coefficient and the curve in Fig.9. Thus, this figure may be used in design problems involving liquefaction or bearing capacity of the soft ground during earthquake.

REFERENCES

Hardin, B.O. and V.P. Drnevich (1970), "Shear Modulus and Damping in Soils," Technical Report, UKY 26-70-CE2.

Hudson, D.E., et al. (1971), "Strong Motion Earthquake Accelerograms, Volume II," Report of Earthquake Engineering Research Laboratory CIT, Part A.

Sato, T. (1975), "Seismic Response of Near-Surface Layer with Non-Linear Characteristics," Annuals, Disaster Prevention Research Institute, Kyoto University, pp.349–365 (in Japanese).

Toki, K. and T. Sato (1976), "Non-Linear Harmonic Wave Propagation in a Layered Ground," Proc. JSCE, No.247, pp.24–34 (in Japanese).